

Full Paper

Calcium Mobilization by Activation of M₃/M₅ Muscarinic Receptors in the Human RetinoblastomaDae-Ran Kim^{1,†}, Sang Hoon Rah^{2,†}, Joon Hyung Sohn³, Byung-Il Yeh³, Chang Mann Ko⁴, Jeong Sook Park¹, Min-Jeong Kim⁵, Joong Woo Lee⁵, and In Deok Kong^{5,*}¹Department of Basic Nursing Science and Institute for Nursing Science, Keimyung University College of Nursing, 194, Dongsan-Dong, Jung-Gu, Daegu, 700-712, Korea²Department of Ophthalmology, ³Department of Biochemistry, ⁴Department of Pharmacology,⁵Department of Physiology and Institute of Lifelong Health, Yonsei University Wonju College of Medicine, 162 Ilsan-Dong, Wonju, Gangwon-Do, 220-701, Korea

Received May 17, 2007; Accepted August 22, 2007

Abstract. Activation of muscarinic acetylcholine receptors (mAChR) is one of the most important signal transduction pathways in the human body. In this study, we investigated the role of mAChR activation in relation to its subtypes in human retinoblastoma cell-lines (WERI-Rb-1) using Ca²⁺ measurement, real-time PCR, and Western Blot techniques. Acetylcholine (ACh) produced prominent [Ca²⁺]_i transients in a repeated manner in WERI-Rb-1 cells. The maximal amplitude of the [Ca²⁺]_i transient was almost completely suppressed by 97.3 ± 0.8% after atropine (1 μM) pretreatment. Similar suppressions were noted after pretreatments with thapsigargin (1 μM), an ER Ca²⁺-ATPase (SERCA) inhibitor, whereas the ACh-induced [Ca²⁺]_i transient was not affected even in the absence of extracellular calcium. U-73122 (1 μM), a PLC inhibitor, and xestospongin C (2 μM), an IP₃-receptor antagonist, elicited 11.5 ± 2.9% and 17.8 ± 1.9% suppressions, respectively. The 50% inhibitory concentration of (IC₅₀) values for blockade of a 100 μM ACh response by pirenzepine and 4-DAMP were 315.8 and 9.1 nM, respectively. Moreover, both M₃ and M₅ mAChRs were prominent in quantitative real-time-PCR. Taken together, the M₃/M₅ subtypes appear to be the major contributor, leading to intracellular calcium mobilization from the internal store via an IP₃-dependent pathway in the undifferentiated retinoblastoma cells.

Keywords: muscarinic receptor, calcium, retinoblastoma

Introduction

Muscarinic acetylcholine receptors (mAChRs) play important roles in regulating the activity of a large number of physiological functions. In mammals, 5 distinct mAChR subtypes (M₁ through M₅) have been identified on the basis of their primary sequences and pharmacological properties (1). Each of the mAChRs requires a specific heterotrimeric G-protein for their respective signaling functions. M₁, M₃, and M₅ receptor subtypes are coupled to G_{α_{q/11}} and G_{α₁₃} subtype G protein, leading to activation of phospholipase C

(PLC) and phospholipase D (PLD), while M₂ and M₄ receptors are preferentially linked to Gi/Go proteins, leading to the inhibition of adenylyl cyclase (2). These patterns of signal transduction of the receptor family subtypes are consistent across tissues, species, and even the states of malignant transformation (2–4).

Cholinergic innervations to the eye are found in all vertebrate classes. Muscarinic M₁–M₅ receptors mediate the metabotropic actions of ACh. The role of muscarinic receptor subtypes has been extensively reviewed in a variety of neuronal and non-neuronal cells (5–7). The selective subtype or subtypes are involved in embryological development, growth or proliferation, oncogenesis, and so on. The diverse functions of the muscarinic receptor subtypes significantly expand their importance in physiology and pathophysiology. Acetylcholine (ACh) is released from autonomic axon terminals or

[†]These authors contributed equally to this paper.

*Corresponding author. kong@yonsei.ac.kr

Published online in J-STAGE

doi: 10.1254/jphs.FP0070877

intrinsic interneurons that make synapses within the retina. Some mAChRs have been found in the human retinal cells, in which mAChRs play one of the most important roles in cellular signaling process (8). Many studies have shown that mAChRs are abundantly expressed and activate intracellular $[Ca^{2+}]_i$ mobilization to regulate cell functions in developing and regenerating retina (8–12).

In the developing vertebrate retina, precise coordination of retinal progenitor cell proliferation and cell-cycle exit is essential for the formation of a functionally mature retina. Unregulated or disrupted cell proliferation may lead to dysplasia, retinal degeneration, or retinoblastoma. Human retinoblastoma, a malignant-changed cell originating from multipotential embryonic retinal cells, is the most common intraocular cancer of childhood (13). Retinoblastoma is associated with inactivating mutations in retinoblastoma protein (Rb), which occurs during mitosis because of errors in DNA replication or mitotic recombination. However, little is known about the human retinoblastoma cell of origin (14). There is now growing evidence that neurotransmitters regulate the proliferation of retinal progenitor cells in the developing retina. One of the interesting things is that the receptor subtypes (M₁–M₅) change with time. For example, the M₄ subtype predominates during the first week of development, while M₃ expression increases moderately and M₂ increases dramatically during the second week of development (15). Also when muscarinic receptor expression in human eye was studied by a number of techniques, the M₃ subtype appeared to be the most abundant. It was reported that high levels of M₃ mRNA have been found in whole eye, retina, iris complex, and sclera (16). However until now, not much is known about the expression profiles of mAChRs, particularly in human retinoblastoma.

Therefore, this study was designed to clarify whether mAChR families are expressed and involved in the changes of intracellular calcium ion concentration. To achieve this goal, we identified mAChR subtypes by using pharmacological and quantitative real-time PCR in the WERI-Rb-1 cells. We found that high levels of M₃- and M₅-subtype mRNAs and proteins were present in the WERI-Rb-1 cells. These M₃/M₅ mAChR appear to be the major contributor leading to intracellular calcium mobilization from the internal store via an IP₃-dependent pathway in the undifferentiated retinoblastoma cells.

Materials and Methods

Cell culture

WERI-RB-1 human retinoblastoma cell lines were purchased from the American Type Culture Collection

(Rockville, MD, USA) and maintained according to the distributor's instructions (17). Briefly, cells were transferred into 25-cm² culture flasks containing 90% RPMI 1640 medium (Cambrex, Walkersville, MD, USA) and 10% fetal bovine serum (GibcoBRL, Grand Island, NY, USA) and grown in a humidified atmosphere with 5% CO₂ at 37°C. Antibiotics (penicillin 100,000 unit/L and streptomycin 100 mg/L) were added to the culture medium. Cells were subcultured again every three to four days. For the experiments, cells were plated on poly-L-lysine coated glass coverslips for 1 h before use.

Fluorescence imaging of $[Ca^{2+}]_i$ in single cells

WERI-Rb-1 cells were loaded with Ca²⁺-sensitive fluorescent dye, Fluo 3-AM (5 μM), at 37°C for 40 min in culture medium. Then, the cells were incubated for an additional 30 min in Fluo 3-AM-free physiological buffer (CaPSS, composition: 145 mM NaCl, 5 mM KCl, 0.8 mM MgCl₂, 1.8 mM CaCl₂, 10 mM HEPES, and 10 mM D-glucose; adjusted to, pH 7.4 with NaOH) at room temperature (24°C–26°C) to remove extracellular traces of the dye and to complete de-esterification. Subsequently, the coverslips were mounted cell-side-up in the free bottom of a perfusion chamber, placed on the stage of an inverted microscope (IX51; Olympus, Tokyo). Throughout the experiments, cells were continuously perfused at approximately 2.0 ml/min by means of a gravity-driven perfusion system with drug-free or drug-containing buffer solutions. In some cases, a Ca²⁺-free buffer was used, which contained 145 mM NaCl, 5 mM KCl, 0.8 mM MgCl₂, 10 mM HEPES, 10 mM D-glucose, 0.1 mM EGTA; adjusted to pH 7.4 with NaOH. The dye-loaded cells were excited at 488 nm by a monochromatic light source (LAMDA DG-4; Sutter, Novato, CA, USA) with 175-W xenon lamp and fluorescence images were captured at 530 nm through an objective lens (40×, UApo/340; Olympus) by an intensified CCD camera (Cascade; Roper, Duluth, GA, USA) controlled by a computer. Fluorescence images were acquired every 1 s during drug applications; however, the interval was increased to every 30 s during recovery or the wash-out period to minimize cell injury from phototoxicity. Data are expressed as DF/F by using MetaFluor 6.1 software package (Universal Imaging Corporation, Downingtown, PA, USA). DF represents the change in fluorescence level of the cells before stimulation, and DF represents the change in fluorescence occurring during stimulation of the cell. All fluorescence measurements were performed at room temperature.

Quantitative real-time RT-PCR

Total cellular RNA was isolated using TriZOL reagent (Invitrogen) according to the manufacturer's

Table 1. Primer sequences for quantitative real-time PCR of M₁, M₃, and M₅ muscarinic receptor subtype

	Primer	Sequence (5' to 3')	Size (bp)	GeneBank Accession #
β -Actin	Sense	AAGTTCACAATGTGGCCGAG	98	NM 001101
	Antisense	ATGGCAAGGGACTTCCTGTA		
M ₁	Sense	CTAGCTGGGCAGTGCTACAT	107	X15263
	Antisense	CAGTAGAGCGTGCACATGAC		
M ₃	Sense	GCCTTCATCATCACTTGGAC	110	U29589
	Antisense	ATGTAGCACAGCCAGTAGCC		
M ₅	Sense	TGCCAGATCCAGTTTCTCTC	110	M80333
	Antisense	TCCCGGTAGATTTCGACAGTA		

protocol. The RNA (1 μ g) was reverse-transcribed and the products were screened by PCR for the presence of cDNA for β -actin, M₁, M₃, and M₅. Real-time PCR was done using the LC system with SYBR Green detection and T_m analysis. SYBR Green (Quagen) was done in a total volume of 10 μ l, which also contained 100 ng of template cDNA and 100 nM of each primer for human muscarinic receptors M₁, M₃, and M₅. PCR Primers were designed using Primer Express software (Applied Biosystems, Foster, CA, USA). Sequences of PCR primers are described in Table 1. Reaction conditions were: 50°C for 2 min and then 95°C for 10 min followed by 45 cycles of 95°C for 30 s, 58°C for 30 s, and 72°C for 30 s. Melting curve analysis was performed to measure the specificity of the PCR product. Each sample was analyzed in triplicate, and data points were used to calculate the average of the three. Positive and negative reference samples were tested along with the unknown samples in each run. Non-specific bands in the PCR product were confirmed by polyacrylamide gel electrophoresis. Relative quantification was performed using the $2^{-\Delta\Delta C_t}$ technique.

Solutions and drugs

WERI-Rb-1 cells were continuously superfused by gravity at a flow rate of 2 ml/min with the bath solution (normal PSS) or experimental solutions. Normal PSS contained 135 mM NaCl, 5 mM KCl, 1.8 mM CaCl₂, 1 mM MgCl₂, 10 mM HEPES, and 10 mM glucose, adjusted to pH 7.4 with NaOH. ACh, atropine, muscarine, methoctramine, thapsigargin, and U-73122 were purchased from Sigma (St. Louis, MO, USA). 4-DAMP and pirenzepine were obtained from Tocris (Ellisville, MO, USA). 4-DAMP and thapsigargin were dissolved into dimethyl sulfoxide (DMSO), and all other drugs were dissolved in distilled water as stock solutions of mM order and stored in a freezer. Each stock solution was diluted to appropriate concentrations with the

Normal PSS just before the start of the experiment.

Statistical significance

Quantitative data are represented as the mean \pm S.E.M. Statistical comparisons were made by the two-tailed *t*-test and ANOVA, and when $P < 0.05$, differences were considered to be significant.

Results

ACh induced a concentration-dependent increase in peak-amplitude cytosolic calcium in the range of 1 – 300 μ M in WERI-Rb-1 cells (EC_{50} was $48.2 \pm 0.1 \mu$ M, Fig. 1). ACh (100 μ M) applied for 60 s produced a sharp Ca²⁺ spike, rapidly increasing within 1 – 2 s on application and immediately recovering after removal of ACh, as shown in Fig. 2A. During repeated applications at 10-min intervals, maximal amplitude of the ACh-induced Ca²⁺ transient elicited minimal desensitization,

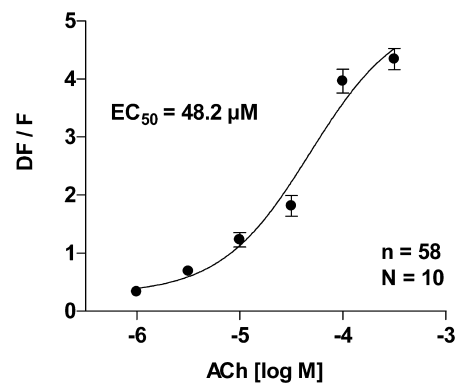


Fig. 1. Concentration-response curve of ACh-induced intracellular Ca²⁺ transients. Data were best fitted using a sigmoid curve derived from Hill's equation with an EC_{50} of 48.2 μ M. Values are each expressed as the mean \pm S.E.M. F: basal fluorescence, DF: maximal amplitude of fluorescence increase, n: total cell number, N: number of experiments.

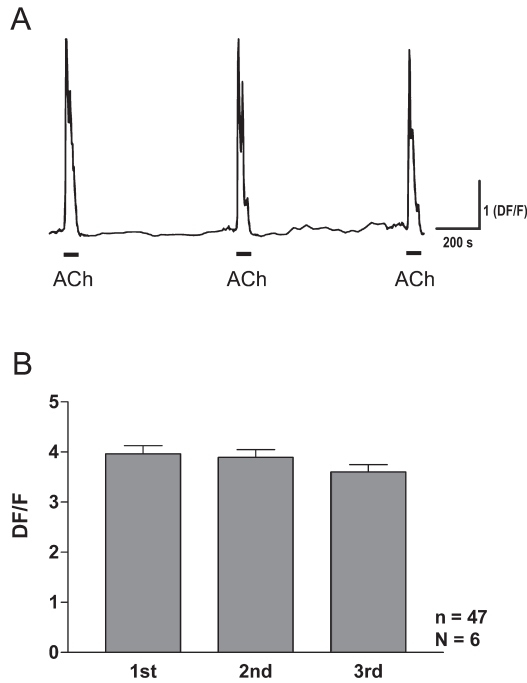


Fig. 2. ACh-induced calcium transient and its stability upon repeated ACh-applications in WERI-Rb-1 cells. A: original time-related traces representing calcium transients after repeated ACh-applications. B: a histogram eliciting maximal amplitudes of calcium transients obtained after repeated ACh-applications ($P = 0.213$). Fluorescent signals were taken up at a speed of 0.1 Hz at room temperature after cells were loaded with 5 μM Fluo-3AM for 1 h at 37°C. ACh (100 μM) was applied for 60 s as indicated by thick bars at 10-min intervals. F: basal fluorescence, DF: maximal amplitude of fluorescence increase, n: total cell number, N: number of experiments.

showing an amplitude about 91% of the first one after the 3rd application (Fig. 2: A and B). Similar responses were obtained in 47 cells ($n = 47$) out of 6 experiments ($N = 6$), which were more than 80% of the cells in the field.

The 100 μM ACh-induced calcium transient was almost completely suppressed by up to $97.3 \pm 0.8\%$ after pretreatment with 1 μM atropine, a nonselective mAChR inhibitor ($n = 92$, $N = 6$, Fig. 3: A and B). Additionally, 100 μM muscarine, a mAChR agonist, also successfully produced a calcium transient with a magnitude similar to that after 100 μM ACh (data not shown). These results indicate that mAChR is involved in the ACh-induced calcium transient in WERI-Rb-1 cells, a cell line from human retinoblastoma.

This calcium transient caused by mAChR was due to Ca^{2+} release from the intracellular Ca^{2+} stores. Figure 4, A and B, showed that the ACh-induced calcium transient was strongly suppressed by pretreatment with 1 μM thapsigargin (TG), which is known to deplete intracellular Ca^{2+} stores by blocking Ca^{2+} -ATPase. TG also

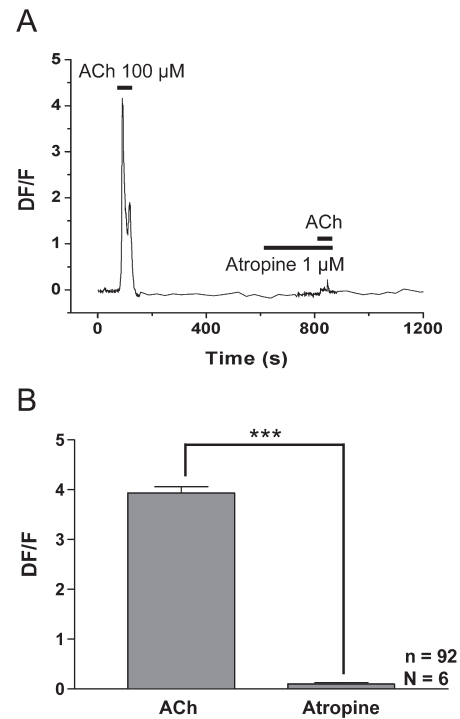


Fig. 3. Effect of atropine on ACh-induced calcium transient in WERI-Rb-1 cells. Original trace (A) and histogram (B) showing a complete suppression of maximal amplitude of 100 μM ACh-induced calcium transient after pretreatment with 1 μM atropine for 3 min. F: basal fluorescence, DF: maximal amplitude of fluorescence increase, n: total cell number, N: number of experiments. *** $P < 0.001$, when compared with Student's *t*-test.

produced a rapid rise of intracellular $[\text{Ca}^{2+}]_i$ within 1 minute, which slowly decayed eventually to the resting level during incubation for 7 min. After that, the ACh-induced calcium transient was markedly attenuated, showing $89.7 \pm 1.5\%$ suppression ($n = 62$), when 100 μM ACh was applied again. We also examined the involvement of external Ca^{2+} influx in the ACh-induced calcium transient by omission of Ca^{2+} in the perfusion solution. ACh-induced calcium transient was independent of the presence of extracellular calcium ions (data not shown).

We further examined the role of the PLC-IP₃ pathway as a mechanism associated with the intracellular calcium mobilization. First, we compared the effect of 1 μM U-73122, a PLC inhibitor, and 1 μM U-73343, an inactive isoform of U-73122. As expected, the maximal amplitude of the ACh-induced calcium transient was suppressed by $88.5 \pm 2.9\%$ after pre-incubation with 1 μM U-73122 ($n = 58$, $N = 5$, Fig. 5: A and B), but not after pre-incubation with 1 μM U-73343 ($n = 40$, $N = 3$, Fig. 5: C and D). In Fig. 6, another approach was preformed to verify the involvement of the PLC-IP₃ pathway by using xestospongine C (2 μM), a membrane-

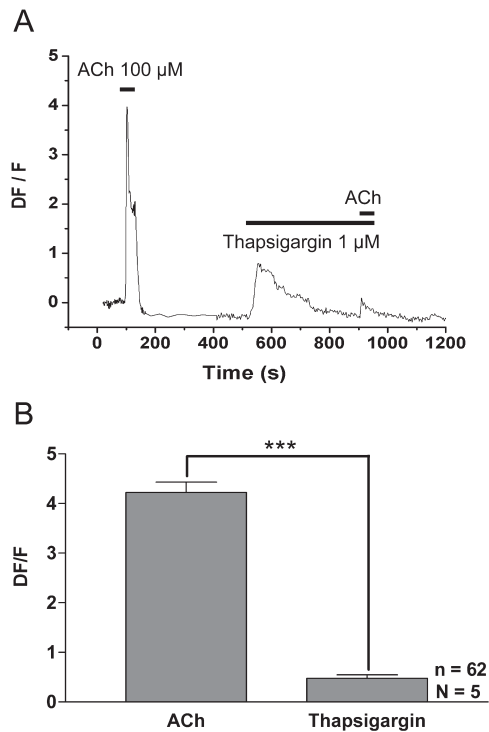


Fig. 4. Effect of thapsigargin on ACh-induced calcium transient in WERI-Rb-1 cells. Original trace (A) and histogram (B) showing an almost complete suppression of maximal amplitude of 100 μ M ACh-induced calcium transient after pretreatment with 1 μ M thapsigargin (TG). Drugs were applied for the given time as indicated by thick bars. F: basal fluorescence, DF: maximal amplitude of fluorescence increase, n: total cell number, N: number of experiments. *** $P < 0.001$, when compared with Student's t -test.

permeable putative IP₃-receptor antagonist. Pre-incubation of xestospongine C for 10 min also strongly suppressed the ACh-induced calcium transient by $82.2 \pm 1.9\%$. These results suggest that muscarinic activation raises $[Ca^{2+}]_i$ by intracellular Ca²⁺ mobilization through the PLC-IP₃ pathway in the undifferentiated retinoblastoma cells.

To further clarify subtypes of mAChR(s), involvement of M₁ receptors was examined by using pirenzepine, a M₁ antagonist, in the WERI-Rb-1 cells. The IC₅₀ value of pirenzepine was 315.8 nM (Fig. 7). On the other hand, that of 4-DAMP, a putative M₁/M₃/M₅-receptor blocker that has preference for the M₃ receptor (18, 19), was 9.1 nM (Fig. 7). The ACh-induced calcium transient was not suppressed by methoctramine (1 μ M), a M₂/M₄ preferred blocker (data not shown). In addition, we also determined the transcript abundance of a single gene among M₁, M₃, and M₅ by relative quantitative real-time PCR. The C_T of each reaction was obtained by using a constant threshold. β -Actin was used as an internal control. ΔC_T was calculated by subtracting the average C_T of β -actin from the average C_T of the

target gene. The relative gene expression was determined as $2^{-\Delta\Delta C_T}$. For the purpose of comparison, M₁ expression in each subtype was set at 1. As shown in Fig. 8, the ratio of relative gene expression for M₁, M₃, and M₅ was 1:6.3:5.6, so M₃ and M₅ were the predominant subtypes, with minor contributions from M₁.

Discussion

In this study, we analyzed the expressional and functional profiles of mAChR subfamilies in WERI-Rb-1 cells, a human retinoblastoma cell-line, by using Ca²⁺ measurement and real-time PCR techniques. Our results showed that M₃- and M₅-mAChR subtypes were predominantly expressed and induced a marked increase in intracellular Ca²⁺ concentration in WERI-Rb-1 cells.

The source of calcium in the calcium transient is either external calcium that enters into the cell through entry channels in the plasmalemma or internal calcium that is released from the internal stores (20). The ACh-induced calcium response obtained in this study elicited a rapid increase and also immediate decrease in its concentration, forming a calcium transient that lasted for less than 1 min, even in the continuous presence of ACh. This calcium transient in the retinoblastoma cells seems primarily due to the internal calcium. This is because the ACh-induced calcium transient was still present after Ca²⁺-omission (data not shown), and it was significantly reduced after depletion of the internal Ca²⁺ stores with TG. It is well known that IP₃ is the major second messenger in the muscarinic signal transduction pathway (11, 21–23). This report showed that the case is the same in the undifferentiated malignant retinoblastoma cells. Basically, the ACh-induced calcium transient was also markedly suppressed after depletion of Ca²⁺ from the internal stores with TG as mentioned above. Additionally, Fig. 6 directly illustrated that the ACh-induced calcium transient was strongly suppressed by preincubation with xestospongine C (2 μ M), a membrane-permeable putative IP₃ receptor antagonist. Furthermore, the ACh-induced calcium transient was also dependent on the PLC as it was markedly suppressed by U-73122, a PLC inhibitor, but not by U-73343, a succinimide analog of U-73122 (24). All these results suggest that the IP₃-PLC pathway is also involved in the ACh-induced Ca²⁺ mobilization in the undifferentiated malignant retinoblastoma cells.

$[Ca^{2+}]_i$ rise is a regulatory signal for many developmental events such as fertilization, embryogenesis and cell proliferation, and even for cell death (20, 25, 26). It has been known that mAChR produces a marked $[Ca^{2+}]_i$ rise in the normal retinal cells in the stages of development (9, 11, 12, 27, 28), differentiation (22), regenera-

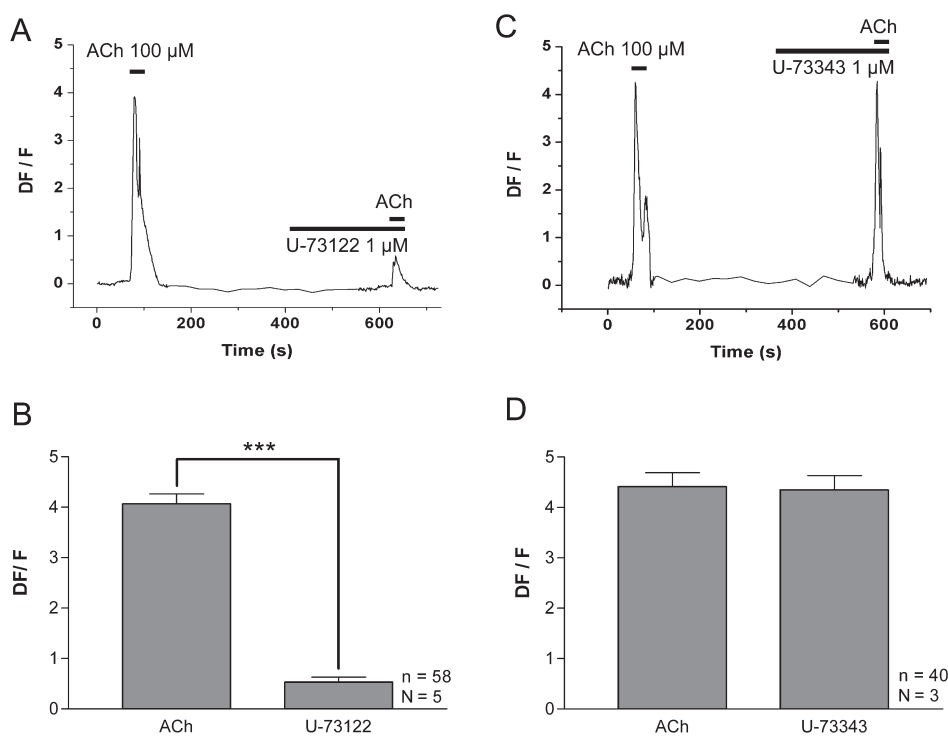


Fig. 5. Differential effect of U-73122 and U-73343 on ACh-induced calcium transient in WERI-Rb-1 cells. Original traces (A and C) and histograms (B and D) showing a strong suppression of maximal amplitude of 100 μ M ACh-induced calcium transient after pretreatment with 1 μ M U-73122, a PLC inhibitor, but not after pretreatment with 1 μ M U-73343, the succinimide analog of U-73122. Drugs were applied for 60 s or for 3 min as indicated by thick bars. F: basal fluorescence, DF: maximal amplitude of fluorescence increase, n: total cell number, N: number of experiments. *** P <0.001 when compared with Student's t -test.

tion (9, 23), and embryo (21). Responsible subtypes for this calcium transient were M₁- and M₃-mAChR subtypes in the retinal cells of human (16), chick embryo (8), and regenerating newt (23). The presence of functionally active M₁- and M₃-mAChR subtypes have also been noted in other tissues of the eye such as human iris (16, 29, 30), ciliary muscle (30), and lens cell and sclera (16), as well as bovine iris (31) and rat exorbital lacrimal acinar cells (32). Additionally, M₂- and M₄-mAChRs and nicotinic acetylcholine receptor (nAChR) have also been noted in the embryonic developmental stage of the retina (9, 33), primitive retinal cells (12, 34), and matured retina (35, 36). However, only the odd numbered muscarinic receptors (M₁, M₃, M₅) were examined in this study because they are directly linked to calcium mobilization.

mAChRs are expressed by amacrine, ganglion, and bipolar and retinal pigmented epithelial (RPE) cells in the adult retina (37–39). Also, calcium imaging studies have further demonstrated that mAChRs are expressed by cells throughout the immature neural retina, including dividing progenitor cells (28). When muscarinic receptor expression in human eye was studied by a

number of techniques, the M₃ subtype appeared to be the most abundant. The quantitative real-time PCR performed by Collins et al. (16) on the whole eye, iris complex, retina, and sclera gave similar results showing that more than 75% of all subtypes of muscarinic receptor was the M₃ receptor, whereas M₁, M₂, M₄, M₅ accounted for less than 10% of the total muscarinic receptors. In addition, it is known that mRNA for M₃ was in greatest abundance in other eye tissues, whereas M₁ was a significant contributor in iris (16). Recently, Liu et al. reported that the M₅-mAChR is abundantly expressed in ocular surface cells such as conjunctival epithelial cells (40). They showed that the amount of mRNA of M₅ subtype was 24 times higher than that of M₁, whereas those of the other four subtypes was not significantly different from one another.

It has been known that the average pK_b values of pirenzepine for M₁ and that of 4-DAMP for M₁/M₃/M₅ are approximately 8 and 9, respectively (18). In our result, the values of pK_b of pirenzepine and 4-DAMP were about 7.0 and 8.5, which were calculated from the Cheng-Prusoff equation (41). This implies that the affinity for 4-DAMP is higher than that of pirenzepine

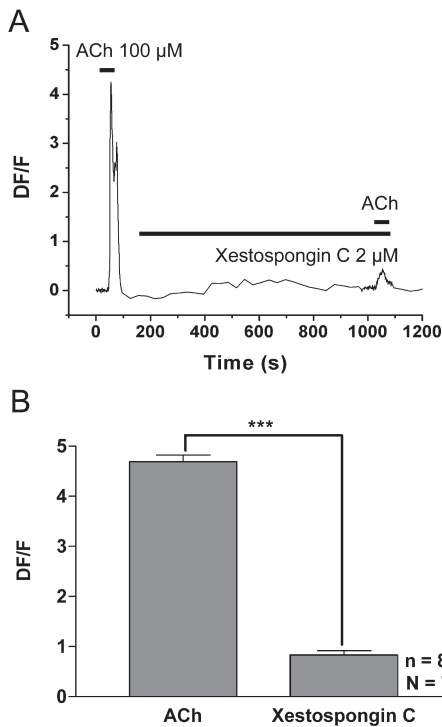


Fig. 6. Involvement of IP₃ receptor in the ACh-induced calcium transient in WERI-Rb-1 cells. Original trace (A) and histogram (B) showing a strong suppression of maximal amplitude of 100 μ M ACh-induced calcium transient after pretreatment with 2 μ M xestospongin C, a selective IP₃-receptor blocker. Drugs were applied for 60 s or for 3 min as indicated by thick bars. F: basal fluorescence, DF: maximal amplitude of fluorescence increase, n: total cell number, N: number of experiments. *** $P < 0.001$, when compared with Student's *t*-test.

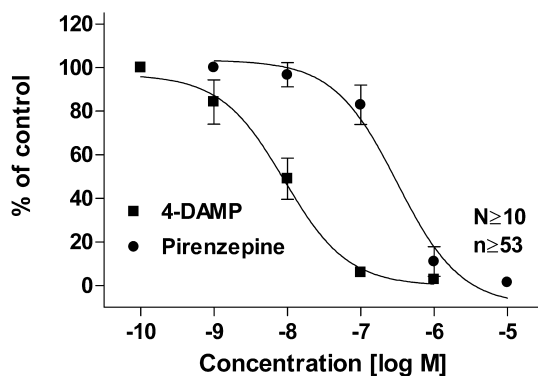


Fig. 7. Inhibition curve of the peak response to ACh by muscarinic antagonists. The inhibitory curves show the peak calcium responses of increasing concentrations of pirenzepine, an M₁-selective antagonist, and 4-DAMP, a selective M₁/M₃/M₅ antagonist, respectively. Data were fitted using sigmoid curves derived from Hill's equation with an IC₅₀ of 316 and 16.1 nM for pirenzepine and 4-DAMP, respectively. Values were each expressed as the mean \pm S.E.M. n: total cell number, N: number of experiments.

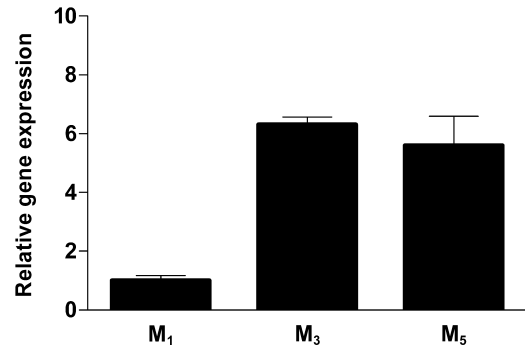


Fig. 8. Relative quantitation of M₁, M₃, and M₅ subtypes by quantitative real-time PCR. Reverse-transcribed products were screened by PCR in the presence of cDNA for β -actin, M₁, M₃, and M₅. Each sample was analyzed in triplicate, and data points were used to calculate the average of the three. Data are each expressed as the mean \pm S.E.M. The relative gene expression M₁, M₃, and M₅ was 1.00 ± 0.17 , 6.31 ± 0.25 , and 5.60 ± 1.1 .

on the retinoblastoma. The lack of M₅-selective agonists and antagonist made it difficult to define the subtype pharmacologically. We attempted to elucidate the levels of the different subtypes in retinoblastoma cells by using quantitative real-time PCR. In our results, the average ratio of M₁, M₃, and M₅ expression levels were 1:6.5:5.6; M₃ and M₅ were predominant relative to M₁, but the relative expression of M₁ was less than 10%. According to the result of this quantitative assay, it is possible that M₃/M₅ could participate in inducing the transient [Ca²⁺]_i rise. However, we could not totally rule out any involvement of the M₁ subtype in calcium mobilization by ACh.

M₅-mAChR is generally identified in discrete brain areas and several peripheral tissues (40, 42, 43). However, the physiological role of M₅-mAChR is still unclear, as no specific antagonist is available yet. Nevertheless, this result may be of value as this is the first demonstration of M₅-mAChR in the human retinoblastoma cell. Furthermore, because odd numbered mAChRs (M₁, M₃, M₅) are linked to calcium mobilization as mentioned earlier, M₅ receptor expressed in retinoblastoma may be a worthwhile novel target for a therapeutic approach to this lethal cancer.

In general, muscarinic agonists reduce proliferation and DNA synthesis in immature rat retinal cultures, while antagonists led to a small increase in proliferation, suggesting that endogenous ACh leads to a negative regulation of cellular proliferation (44). The potential role of muscarinic stimulation on the proliferation needs to be further investigated in human retinoblastoma.

In summary, using pharmacologic and molecular techniques, we showed that in retinoblastoma M₃- and M₅-mAChR subtypes are prominent relative to M₁,

which induces a transient $[Ca^{2+}]_i$ rise primarily through a Ca^{2+} release from intracellular stores. This conclusion will serve as a clue to understanding the roles of mAChRs in the regulation of cellular functions in retinoblastoma.

Acknowledgment

This research was supported by the Regional Innovation Center Program, which was conducted by the Ministry of Commerce, Industry and Energy of the Korean Government.

References

- Caulfield MP, Birdsall NJM. International Union of Pharmacology. XVII. Classification of muscarinic acetylcholine receptors. *Pharmacol Rev.* 1998;50:279–290.
- Caulfield MP. Muscarinic receptors – characterization, coupling and function. *Pharmacol Ther.* 1993;58:319–379.
- Hosey MM. Diversity of structure, signaling and regulation within the family of muscarinic cholinergic receptors. *FASEB J.* 1992;6:845–852.
- Felder CC. Muscarinic acetylcholine receptors: signal transduction through multiple effectors. *FASEB J.* 1995;9:619–625.
- Felder CC, Bymaster FP, Ward J, Delapp, N. Therapeutic opportunities for muscarinic receptors in the central nervous system. *J Med Chem.* 2000;43:4333–4353.
- Eglen RM. Muscarinic receptor subtypes in neuronal and non-neuronal cholinergic function. *Auton Autacoid Pharmacol.* 2006;26:219–233.
- Nouchi H, Kaeriyama S, Muranatsu A, Sato M, Hirose K, Shimizu N, et al. Muscarinic receptor subtypes mediating positive and negative iontophy in the developing chick ventricle. *J Pharmacol Sci.* 2007;103:75–82.
- Belmonte KE, McKinnon LA, Nathanson NM. Developmental expression of muscarinic acetylcholine receptors in chick retina: selective induction of M2 muscarinic receptor expression in ovo by a factor secreted by muller glial cells. *J Neurosci.* 2000;20:8417–8425.
- Cheon EW, Kuwata O, Saito T. Muscarinic acetylcholine receptors in the normal, development and regenerating newt retinas. *Dev Brain Res.* 2001;127:9–21.
- Oettling G, Schmidt H, Show-Klett A, Drews U. Expression of the Ca^{2+} mobilizing muscarinic system in the chick embryo correlates with morphogenesis. *Cell Diff.* 1988;23:77–86.
- Yamashita M, Yoshimoto Y, Fukuda Y. Muscarinic acetylcholine responses in the early embryonic chick retina. *J Neurobiol.* 1994;25:1144–1153.
- Wong ROL. Cholinergic regulation of $[Ca^{2+}]_i$ during cell division and differentiation in the mammalian retina. *J Neurosci.* 1995;15:2696–2706.
- McFall RC, Nagy RM, Nagle BT, McGreevy LM. Scanning electron microscopic observation of two retinoblastoma cell lines. *Cancer Res.* 1978;38:2817–2835.
- Dyer MA, Bremner R. The search for the retinoblastoma cell of origin. *Nat Rev Cancer.* 2005;5:91–101.
- Nadler LS, Rosoff ML, Hamilton SE, Kalaydjian AE, McKinnon LA, Nathanson NM. Molecular analysis of the regulation of muscarinic receptor expression and function. *Life Sci.* 1999;64:375–379.
- Collison DJ, Coleman RA, James RA, Carey J, Duncan G. Characterization of muscarinic receptors in human lens cells by pharmacologic and molecular techniques. *Invest Ophthalmol Vis Sci.* 2000;41:2633–2641.
- Barnes S, Haynes LW. Low-voltage-activated calcium channels in human retinoblastoma cells. *Brain Res.* 1992;11:19–22.
- Eglen RM, Watson N. Selective muscarinic receptor agonist and antagonist. *Pharmacol Toxicol.* 1996;78:59–68.
- Watson N, Daniels DV, Ford AP, Eglen RM, Hegde SS. Comparative pharmacology of recombinant human M3 and M5 muscarinic receptors expressed in CHO-K1 cells. *Br J Pharmacol.* 1999;127:590–596.
- Berridge MJ. Calcium signal transduction and cellular control mechanisms. *Biochemical Biophys Acta.* 2004;1742:3–7.
- Sakaki Y, Fukuda Y, Yamashita M. Muscarinic and purinergic Ca^{2+} mobilizations in the neural retina of early embryonic chick. *Int J Dev Neurosci.* 1996;14:691–699.
- Naruoka H, Kojima R, Ohmasa M, Layer PG, Saito T. Transient muscarinic calcium mobilization in transdifferentiating as in reaggregating embryonic chick retinae. *Dev Brain Res.* 2003;143:233–244.
- Omama M, Saito T. Muscarinic calcium mobilization in the regenerating retina of adult newt. *Dev Brain Res.* 2003;145:61–69.
- Bleasdale JE, Fisher SK. Use of U-73122 as an inhibitor of phospholipase C-dependent processes. *Neuroprotocols.* 1993;3:125–133.
- Ciapa B, Pesando D, Wilding M, Whitaker M. Cell-cycle calcium transients driven by cyclic changes in inositol triphosphate levels. *Nature.* 1994;368:875–878.
- Berridge MJ, Bootman MD, Lipp P. Calcium—a life and death signal. *Nature.* 1998;395:645–648.
- Yamashita M, Sugiyama M. Calcium mobilization systems during neurogenesis. *News Physiol Sci.* 1998;13:75–79.
- Pearson R, Catsicas M, Becker D, Mobbs P. Purinergic and muscarinic modulation of the cell cycle and calcium signaling in the chick retinal ventricular zone. *J Neurosci.* 2002;22:7569–7579.
- Ishizaka N, Noda M, Yokoyama S, Kawasaki K, Yamamoto M, Higashida H. Muscarinic acetylcholine receptor subtypes in the human iris. *Brain Res.* 1998;787:344–347.
- Zhang X, Hernandez MR, Yang H, Erickson K. Expression of muscarinic receptor subtype mRNA in the human ciliary muscle. *Invest Ophthalmol Vis Sci.* 1995;36:1645–1657.
- Honkanen RE, Howard EF, Abdel-Latif AA. M3-muscarinic receptor subtype predominates in the bovine iris sphincter smooth muscle and ciliary processes. *Invest Ophthalmol Vis Sci.* 1990;31:590–593.
- Mauduit P, Jammes H, Rossignol B. M3 muscarinic acetylcholine receptor coupling to PLC in rat exorbital lacrimal acinar cells. *Am J Physiol.* 1993;264:C1550–C1560.
- McKinnon LA, Nathanson NM. Tissue-specific regulation of muscarinic acetylcholine receptor expression during embryonic development. *J Biol Chem.* 1995;270:20636–20642.
- Lecchi M, Marguerat A, Ionescu A, Pelizzone M, Renaud P, Sommerhalder J, et al. Ganglion cells from chick retina display multiple functional nAChR subtypes. *Neuroreport.* 2004;15:

- 307–311.
- 35 Strang CE, Amthor FR, Keyser KT. Rabbit retinal ganglion cell responses to nicotine can be mediated by beta2-containing nicotinic acetylcholine receptors. *Vis Neurosci.* 2003;20:651–662.
- 36 Moretti M, Vailati S, Zoli M, Lippi G, Riganti L, Longhi R, et al. Nicotinic acetylcholine receptor subtypes expression during rat retina development and their regulation by visual experience. *Mol Pharmacol.* 2004; 66:85–96.
- 37 Hutchins JB, Hollyfield JG. Acetylcholine receptors in the human retina. *Invest Ophthalmol Visual Sci.* 1985;26:1550–1557.
- 38 Hutchins JB. Development of muscarinic acetylcholine receptors in the ferret retina. *Brain Res Dev Brain Res.* 1994;82:45–61.
- 39 Fischer AJ, McKinnon LA, Nathanson NM, Stell WK. Identification and localization of muscarinic acetylcholine receptors in the ocular tissues of the chick. *J Comp Neurol.* 1998;392:273–284.
- 40 Liu S, Li J, Tan DTH, Beuerman RW. Expression and function of muscarinic receptor subtypes on human cornea and conjunctiva. *Invest Ophthalmol Visual Sci.* 2007;48:2987–2996.
- 41 Craig DA. The Cheng-Prusoff relationship: something lost in the transition. *Trends Pharmacol Sci.* 1993;14:89–91.
- 42 Bonner TI, Buckley NJ, Young AC, Brann MR. Identification of a family of muscarinic acetylcholine receptor genes. *Science.* 1987;31:527–532.
- 43 Peralta EG, Ashkenazi A, Winslow JW, Smith DH, Ramachandran J, Capon DJ. Distinct primary structures, ligand-binding properties and tissue-specific expression of four human muscarinic acetylcholine receptors. *EMBO J.* 1987;20:3923–3929.
- 44 dos Santos AA, Medina SV, Sholl-Franco A, de Araujo EG. PMA decreases the proliferation of retinal cells in vitro: the involvement of acetylcholine and BDNF. *Neurochem Int.* 2003;42:73–80.